Cost effective and reliable electric wire filaments coated with nanofabricated and sintered superconductive ceramics

A. Rokhvarger*

This paper reports the major results of research and development of thermochemically nanofabricated high temperature superconducting (HTS) ceramic leads and multifilament HTS $YBa_2Cu_3O_{7-x}$ (HTS-YBCO) electric wire. Advanced scientific features of the created ceramic engineering processing based on ceramic polymer (silicone) nanotechnology, including ceramic coating on continuous metal filaments, are discussed. Thermochemical nanofabrication of the honeycomb-like nanoarchitecture resulted in intergrain superconductivity of the fully dense sintered YBCO macroceramics, which is close to the inner grain superconductivity of the initial YBCO particles. The developed multifilament HTS-YBCO wire is cost effective, reliable, flexible and as workable as copper wire, but conducts ~100 times more electricity with insignificant heat losses.

Keywords: YBCO ceramics, Silicone polymer, Adhesion coating, Nanofabrication, Nanoarchitecture, Superconductive wire

This paper is part of a special issue on Novel Advanced Ceramic and Coating Processing

Introduction

Superconductivity was discovered over 100 years ago and was observed in some metals and alloys that are superconducting at very low temperatures achieved by liquid helium coolant, which makes their application very expensive and limited. About 25 years ago, the fifth superconductivity related Nobel Prize in Physics[1–3] was awarded for the discovery of high temperature superconductor (HTS) cuprate ceramic particles. Some cuprates can be superconducting at temperatures higher than the boiling temperature of inexpensive and safe liquid nitrogen (LN), or 77 K. This resulted in great potential for broad commercial application of HTS ceramic leads, since the required cryogenic conditions could now be efficiently provided by the Gifford/MacMahon refrigeration machine.

The most marketable and anticipated product is HTS electric wire, which is the major material of power transmission and end use equipment, such as electric cables, motors, transformers and generator rotors. Additionally, inexpensive and reliable HTS round wire would make possible design and exploitation of new and advanced systems, including superpower jet propulsion magnetic engines for ships and aero- and space vehicles and magnetic resonance imaging medical systems.[5]

During a 25 year worldwide effort, scientists used mechanical engineering methods developing 'first generation' oxide powder loaded in silver tube HTS wire (1G HTS wire) and 'second generation' template film deposition (TFD) of HTS ceramic crystals on multimetal layered tape with biaxially nanotextured surface (2G HTS tape).[6] However, 1G and 2G HTS wires are uncompetitive with ordinary copper and aluminium electric wires due to innate quality, reliability and workability drawbacks and high capital and production costs.[7–10]

The HTS polycrystalline ceramic leads consist of a plurality of nanosize HTS ceramic grains. The 25 year old and key technological problem is how to treat initial nanosize HTS crystals to achieve intergrain superconductivity within the entire macroceramic body, which has to be equal or close to the superconductivity of the initial ceramic grains.

We provided thermochemical technological manipulations of $YBa_2Cu_3O_{7-x}$ (YBCO) nanosize crystals,[11,12] which allowed development of the ceramic engineering method to manufacture a 'third generation' (3G) HTS round wire, as opposed to mechanical engineering methods of 1G wire and 2G HTS tape technologies. The research resulted in the nanofabrication of sintered YBCO coated metal filaments that are reflected in numerous publications and US patents.[13–23]

Thermochemical nanofabrication of HTS ceramic coated filaments

Experiments were conducted at the Polytechnic Institute of New York University. The development of 3G HTS ceramic processing method began with the selection of raw materials and was followed by six nanotechnological stages: preparation of raw material mixture, product forming, magnetic grain orientation, polymerisation hardening, ceramic firing and product customisation.

3G HTS Corporation, NY, USA, www.3GHTS.com

*Corresponding author, email aerokhv@verizon.net

Received 20 December 2011; accepted 28 February 2012
DOI 10.1179/1743676112Y.0000000027

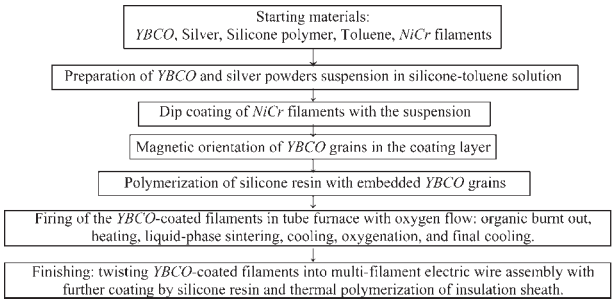

1 Flow chart of conveyor nanofabrication of multifilament 3G HTS electric wire

Figure 1 shows a flow chart of the developed method of conveyor nanofabrication of multifilament 3G HTS electric wire.

Starting materials

The starting materials for the nanofabrication of 3G HTS macroceramics consisted of a major component and two additives. The major component was YBCO superconductor ceramic nanopowder produced by Superconductive Components, Inc., OH, USA. Superconductive Components, Inc. developed a method of coprecipitation solution of Y, Ba, and Cu salts.[24] The YBCO powder was supplied with particle size 500–1000 nm (0·5–1 μm), melting point in air ~1000°C and critical temperature T_C ~92 K.

It should be noted that the patented 3G HTS nanotechnology allowed the use of any oxide or non-oxide superconducting ceramic particle, for example, MgB_2 or iron pnictide HTS particles, but the YBCO ceramics demonstrate at LN temperature the best electromagnetic properties.[10]

The first additive was silver (Ag) nanosize powder added in the amount of 2–3 wt-%. The second additive was 3–5 wt-% of liquid silicone polymer with molecular weight 30 000–40 000, HO–[–Si$(CH_3)_2$O–]–H. Silicone is an off the shelf available and inexpensive product and was received from Gelest, Inc. (PA, USA). Only silicone polymers include both organic and inorganic (Si) components, which provide unique opportunities for nanoceramic engineering. The silicone polymer emulsion in toluene solvent does not react with HTS ceramic crystals and coats them, thus protecting from air and water degradation during further technological processing.

The developed technology uses flexible filament substrates such as quartz glass, glass carbon, Ag and NiCr alloy. They are stable at ceramic sintering temperatures and do not destroy the superconductivity of HTS ceramics. The best choice was off the shelf available NiCr filaments that are inexpensive, firm, flexible, corrosion and creep resistant and do not react with YBCO ceramics.

Preparation of raw material mixture

The wet ceramic processing method was used. The YBCO and silver powders were mixed by a mechanical mixer with silicone emulsion in a toluene solvent and homogenised by an ultrasonic device. Ultrasonic impact disaggregated YBCO microparticles to nanosize grains. Finally, a homogeneous suspension of YBCO and Ag nanoparticles in silicone emulsion was produced.

Product forming

The resulting suspension can be used for slip casting, coating other surfaces and printing of circuits. A condensed suspension can be used for pressing or extrusion.

To achieve high flexibility of continuous HTS wire, the YBCO ceramics should have a thickness below 30 μm. A dip coating method[25,26] employing adhesion effect was used, allowing the formation of a ceramic coating with a thickness 9–12 μm on continuous and flexible substrate filaments.

A NiCr alloy filament substrate of 40 μm in diameter was submerged and moved through a vessel with raw material suspension mixture in silicone emulsion, which has glue properties. The fine powder suspension adhered to the filament substrate. The coating thickness was controlled by suspension viscosity and the velocity of the movement of the filament through a vessel.

At constant process parameters (temperature, suspension viscosity, adhesion time and diameter and properties of the substrate filament), the long length thickness of the adhered YBCO ceramic layer will be constant, which is a very important practical advantage in comparison with 2G HTS tape techniques.

Magnetic grain orientation

Magnetic grain orientation was conducted immediately after the ceramics coating was formed. Most ceramics are dielectric materials. Compared to that, YBCO crystals are good electrical conductors and respond to an applied magnetic field as iron.

Using this phenomenon, the filaments coated with a soft layer of YBCO grains were moved between poles of 0·3 T permanent magnet, resulting in the rotation and uniform orientation of *a*–*b* planes of YBCO crystal lattices along the filament length (in the direction of the electric flux).

Polymerisation hardening

Next applied was the polymer chemistry method consisting of polymerisation hardening of silicone in silicone ceramic composite. The curing was conducted in open air, for a few hours, or in an oven at gradually raised temperatures up to 200°C.

Ceramic firing

A tube furnace with a programmable controller was used. Oxygen was blown through the furnace in the direction opposite the direction of filament movement.

The high temperature thermochemical processing in the tube furnace took 30–40 h and consisted of six consecutive steps: slow heating up to 550°C for organic burn out, fast heating to sintering temperature 920–935°C, liquid phase ceramic sintering, fast cooling to 550–600°C, oxygenation of YBCO crystals to restore oxygen stoichiometry at 420–460°C (dwelling ~1·5 h) and final cooling.

After sintering shrinkage, the YBCO ceramic coating layer was 7–9 μm thick. The YBCO coating layer consists of one superconductive and two non-superconductive sublayers that, together with a metal filament substrate, decrease the superconductivity of the entire cross-section of the electric wire. The non-superconductive sublayers are: ~1 μm thick of the metal–ceramics mutual diffusion bonding layer and ~1 μm thick of the surface layer, which can have grooves interfering electric flux.

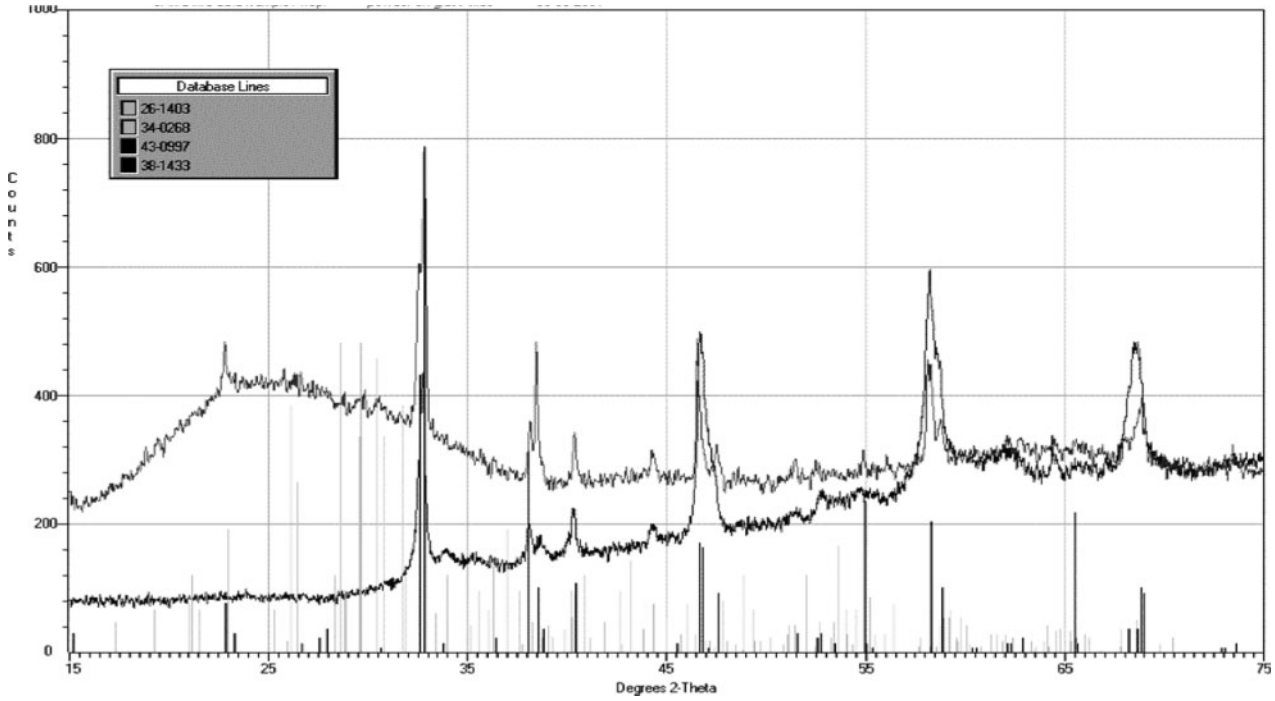

2 Two X-ray difractograms of cured amorphous silicone polymer filled with YBCO grains (lower pattern) and sintered YBCO composite ceramics (upper pattern)

Finishing

The 3G HTS filaments can be woven (twisted), for example, into 2 or 4 filament assemblies similar to multifilament copper wire broadly used for various electrical engineering applications.

Using the dip coating or pulverisation methods, 3G HTS filament assembly providing a customised electric wire can be coated with an emulsion of silicone rubber insulation material.[21] Polymer resin cured at temperatures up to 250°C does not breach the superconductivity of sintered YBCO ceramics. The silicone insulator can provide inexpensive and reliable mechanical protection of 3G HTS wire or cable at room and cryogenic temperatures.

Nanofabrication of superconductive nanoarchitecture of sintered HTS macroceramics

Phase transformation

The organic part of the silicone polymer HO–[–$Si(CH_3)_2O$–]–H was burned out during the heating process while the inorganic silicon element residuals were located in the grain boundary areas of the YBCO material. At sintering temperatures of 920–935°C, silicon elements react with a small number of YBCO crystals and silver, forming a multicomponent eutectic melt. During the fast liquid phase sintering, this melt fills the grain boundary nanothick size gaps. After cooling, the melt forms solid glass films that provide integrity of the sintered YBCO ceramics. The presence of Ag makes the glass films electroconductive.

Differential thermal analysis, X-ray and microscopic studies (optical and SEM) of the YBCO composite coating before and after tube furnace firing were used to study the changes in YBCO ceramic composite during processing.[27]

Figure 2 shows two superimposed X-ray diffractograms. The lower pattern of the cured silicone YBCO material before firing shows the presence of only YBCO peaks. The upper pattern of the sintered YBCO composite ceramics indicates the presence of glass phase with signs of devitrification of glass. All YBCO peaks on both X-ray patterns coincide, which indicates that after firing YBCO crystals retain their initial structure and, therefore, superconducting properties.

X-ray and microscopic studies identified two components of the sintered YBCO composite ceramics: YBCO grains (crystalline phase) and multicomponent glass films (glass phase) located in the grain boundary areas. The glass films provide the electromagnetic vortex pinning centres and electrical percolation network, which facilitates intergrain superconductivity of YBCO composite ceramics.

Structural evolution

Optical, electron and atomic force (AFM) microscopies were used to observe[28] at nanometre and micrometre magnifications the nanostructural evolution of YBCO ceramics, which was induced by nanotechnological forming, polymerisation and sintering processes.

The polymerisation results in a homogeneous three-dimensional (3D) crosslinked polymer matrix (Fig. 3). This matrix can form a honeycomb-like uniform 3D nanoscaffold for embedded YBCO grains. This homogeneously oriented structure is retained in the sintered YBCO composite ceramics, as shown in Figs. 4 and 5.

The sintering process fixes the positions of equally sized and uniformly oriented YBCO grains (honeycomb cells) in frames consisting of glass films located in nanothin grain boundary areas (walls of 3D scaffold). There is a uniform and homogeneous honeycomb-like two phase nanoscale structure within the sintered macrosize ceramic body.

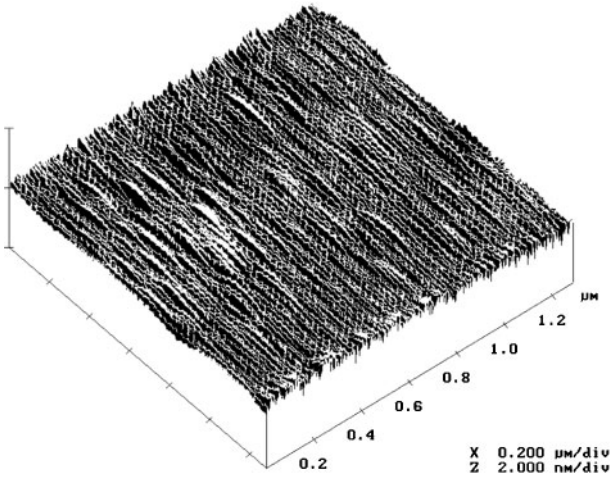

3 Three-dimensional AFM surface image of cross-linked matrix of cured silicone polymer

Nanoarchitecture of superconductive ceramics

The nanofabrication technique allowed to obtain a fully dense sintered YBCO ceramic composite with homogeneous honeycomb-like nanoarchitecture of uniformly oriented and completely aligned YBCO crystal grains with an orthorhombic crystal structure (major superconducting phase) and a uniform 3D network of multicomponent nanothick glass films (minor superconductivity supporting phase) located in the grain boundary areas of YBCO grains.

Having this 3D nanoarchitecture, the YBCO macroceramics provide a homogeneous network of Abrikosov/Josephson magnetic flux vortex pinning centres[2,3] and make possible Josephson and weak tunnelling,[29] electrical percolation,[30] gossamer superconductivity,[31] proximity[32] and other intergrain superconducting effects[33,34] that cause macroscale superconductivity of the sintered polycrystalline (granular) YBCO ceramic leads.

Superconductivity measurements

Superconductivity of 3G HTS ceramics

Electrical current resistance (Fig. 6) and magnetic susceptibility (Fig. 7) versus cryogenic temperature on slip cast and sintered centimetre size plate of 3G HTS ceramics were measured.

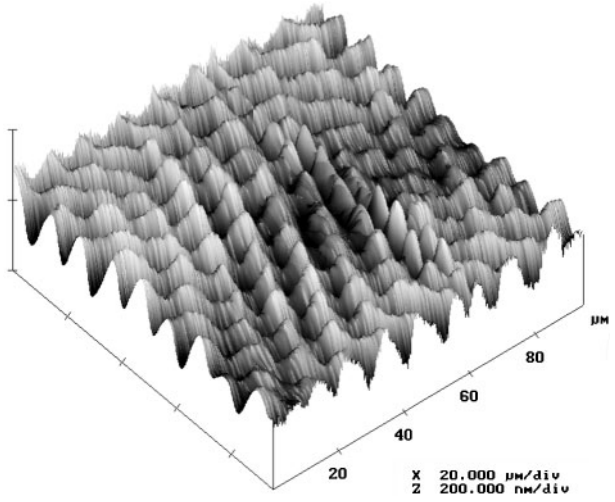

5 Three-dimensional AFM surface image of sintered YBCO coating on alumina substrate (at micro- to nano-size scale)

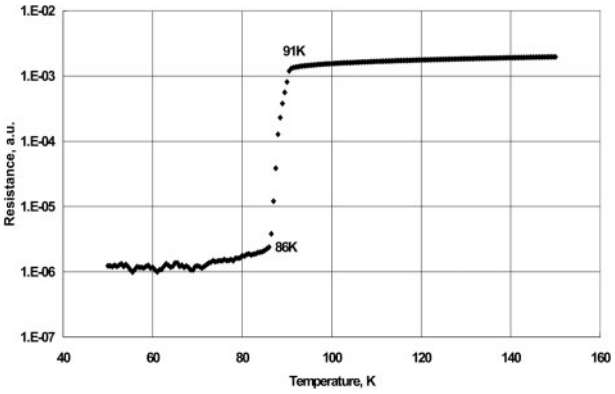

6 Electrical current resistance (in arbitrary units) versus temperature measured on slip cast and sintered centimetre size plate of YBCO ceramics

As shown in Figs. 6 and 7, the nanofabricated YBCO composite is a superconductor that changes from paramagnetic to diamagnetic state within a transition temperature zone,[2,3] i.e. 84–91 K. This zone is slightly different from the transition zone for pure YBCO grains.[2,3] However, these temperatures are higher than the boiling temperature of the LN coolant, i.e. 77 K.

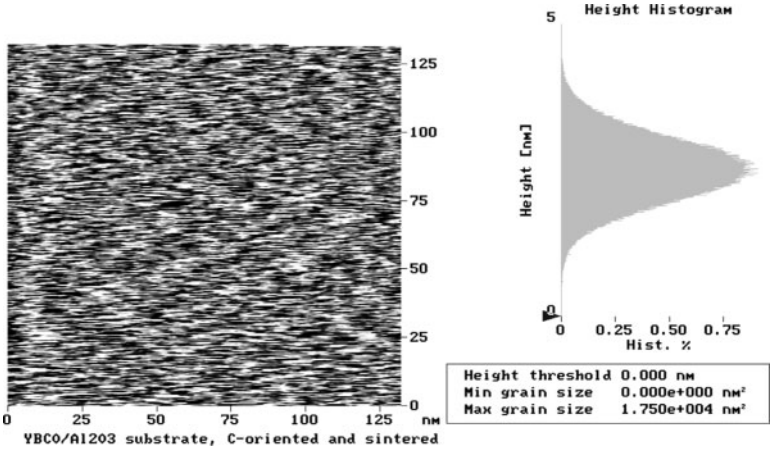

4 Two-dimensional AFM surface image and grain height histogram of sintered YBCO coating on alumina substrate: lengths of uniformly oriented and aligned YBCO grains are 15–20 nm

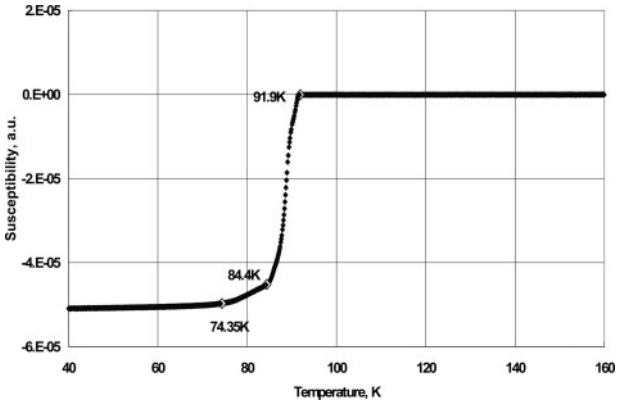

7 Magnetic susceptibility (in arbitrary units) versus temperature measured on slip cast and sintered centimetre size plate of YBCO ceramics

The applied magneto-optical visualisation technique[35,36] allowed the determination of light refraction as a function of the penetration or magnetic susceptibility of the raised magnetic field in the sintered YBCO macroceramic samples at cryogenic temperatures. When the magnetic field was raised, the appearance, at certain magnetic field density, of ripple zones on the light transparent microsize in plane sample corresponds to a certain critical value of the electric current carrying capacity J_C at practically zero resistance (virtually no heat loss) of the YBCO ceramics.

On 1 μm side square of the centimetre size slip cast and sintered YBCO ceramic composite plate, the estimated critical value of electric current passing through the ceramic sample was $J_C \sim 10^9$ A cm^{-2} at 65 K. This value on the mesoscale level current density of the YBCO ceramic composite is close to the maximum achievable J_C of the nanosize YBCO ceramic crystal grains. This demonstrated superior efficiency of the developed nanotechnology and superior intergrain superconductivity of the 3G HTS-YBCO ceramics.

The superconductivity of the nanofabricated 3G HTS-YBCO pellets was also proven by demonstration of the powerful Meissner effect (Fig. 8).

Superconductivity of 3G HTS electric wire

The four point method, which is recommended for electrical and electronic engineers by the American Standard Testing Methods and the International Electro-Technical Commission, was applied to measure the volt–ampere characteristics of the tested electric wire at LN temperatures. The engineering densities of the electric current transmitted at corresponding voltages through the entire silver and 3G HTS-YBCO filament cross-sections J_E (kA cm^{-2}) were measured and compared. It showed the superconductivity of 3G HTS-YBCO filaments.

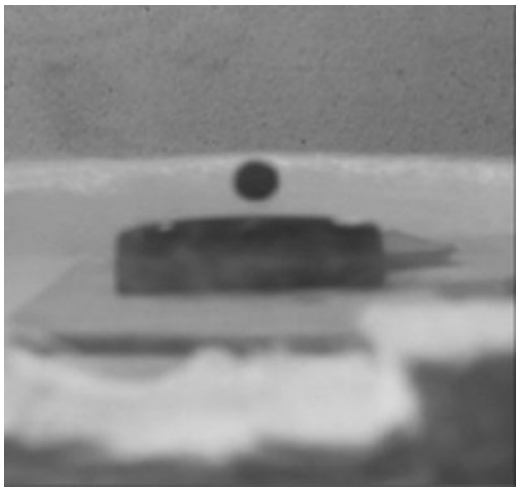

8 Photograph of rare earth magnet tablet (5 mm diameter and 1·5 mm thickness) levitating 7 mm above dry pressed and sintered YBCO ceramic disc (30 mm diameter and 2 mm thickness) immersed in LN

Then, J_E of the 3G HTS-YBCO filaments was measured at direct current (dc) voltages and insignificant heat losses normally applied in electrical engineering and electronics end use systems and devices.[4,8] As shown in Table 1, the tested 3G HTS-YBCO filaments on Ag and NiCr substrates demonstrated at LN temperature J_E values that are >100 times higher than J_E of copper filaments at room temperature and the same voltages and insignificant heat losses used correspondingly for electrical engineering or electronics applications. This sure puts 3G HTS-YBCO filaments in the range J_E=10–20 kA cm^{-2} (77 K, self-field, 1 μV cm^{-1} of the dc), which the Electric Power Research Institute, Palo Alto, CA, USA, determined as the most efficient for electrical engineering applications of HTS wire.

Advantages of 3G HTS electric wire

Reliability

The fully dense sintered 3G HTS macroceramics have high strength, integrity and thermodynamic stability that prevent air degradation of individual HTS grains. Glass films actually encapsulate YBCO grains, preventing their contact with outside air or a coolant agent and, therefore, assuring chemical reliability and durability of the sintered YBCO ceramics and 3G HTS wire.

Spontaneous quenches of superconductor current flux[37] are an innate problem for thin HTS films that are deposited on 2G HTS tape with working thickness of the HTS ceramics ~0·3 μm. The quenches were not observed for bulk HTS ceramic leads and 3G HTS filaments with

Table 1 Electric current densities J_E for copper wire (at room temperature) and two 3G HTS-YBCO filaments (at LN temperature) measured at same dc voltages and insignificant heat losses

Properties and characteristics	Electrical engineering applications	Electronic applications
Typical working conditions of electric copper wire		
Assigned value of expending power/W cm^{-3}	1	0·1
Used voltage in engineering systems with copper wire/V cm^{-1}	0·005	0·0005
Applied electric current density transmitted through wire J_E/A cm^{-2}	200	200
Measured J_E on 3G HTS-YBCO filament samples		
A filament with Ag substrate/A cm^{-2}	33 536	4090
A filament with NiCr substrate/A cm^{-2}	28 644	3643

YBCO coating layer thickness of about 7–9 μm thick. It is assumed that at such thickness of HTS ceramic leads the crystal scale quench breaches of the electric current flux should be momentarily compensated by the number of neighbouring HTS ceramic grains that can transmit the entire electrical current flux. This prevents overheating of neighbour crystals and makes multifilament 3G HTS electric wire quench reliable.

Additionally, in case of temporary breaches of superconductivity of the woven with each other filament of 3G HTS wire, switch the electric current from one to another, compensating these breaches.

The nanofabricated and sintered YBCO composite ceramics and 3G HTS wire filaments with NiCr substrate demonstrated at room temperature a silver-like electric current carrying capacity J_E. This increases the reliability of 3G HTS wire in case of a lack of coolant or a breach in transmission system.

Other advantages

Thermochemical 3G HTS nanotechnology provides the following key advantages of YBCO coated filaments and multifilament 3G HTS electric wire:

(i) in comparison with tape, the round shape of filaments provides up to five times increase in magnetic susceptibility. This can decrease cost and simplify HTS cable design and makes the use of this wire in coils of electric motors, transformers and generator rotors efficient
(ii) contacting with each other, YBCO ceramic coated filaments provide self-magnetic shielding, which simplifies multifilament 3G HTS wire and cable design and makes them less expensive
(iii) multifilament design makes splicing 3G HTS wire and cable segments feasible. This is similar to copper wire splicing workability
(iv) available bending radii defining the flexibility of NiCr substrate filaments coated by sintered YBCO ceramics are small enough to provide traditional manipulations with electric wire and cable
(v) the invented and developed thermochemically self-controlled ceramic nanofabrication method assures quality and repeatability of all characteristics of 3G HTS electric wire
(vi) the invented conveyor technique includes the tube oven for composite polymerisation, tube furnace for ceramic firing and the fully mechanised filament handling system. This technique provides cost effective continuous '[a substrate filament reel] – to – [an HTS filament reel]' manufacturing of 3G HTS wire
(vii) assigning the number of twisted YBCO filaments, one can make 3G HTS electric round wire or cable of any required diameter and electric current carrying capacity
(viii) inexpensive insulation of 3G HTS wire and cables by silicone polymer resin sheath, which is stable in air and at cryogenic temperatures.

Cost efficiency

The cost/performance ratio, *C*/*P*, is the major marketing characteristic of electric wire. The *C*/*P* of 3G HTS round wire is US$5–7/kAmp-m (for 1 m length of wire with 1 cm^2 cross-section). The *C*/*P* of electric copper wire varies in the range US$15–55/kA-m while the *C*/*P* of 2G HTS wire is US$75–100/kA-m.

The estimated production cost of the thinnest 3G HTS filament with a diameter of 0.06 mm is US$0.50 per meter. This elementary 3G HTS filament can transmit electricity as electric copper wire with a diameter 6 mm and a market price US$5–20 per meter.

The capital cost of mechanical equipment, a long-length electrical tube oven and furnace, and filament handling system of the typical industrial line should be 5–10 times less than the capital cost of the equipment required for manufacturing 1G and 2G HTS wires.

Summary

The major phenomena and principles controlling the transfer of nanoscale inner crystal superconductivity to intergrain levels of 3D HTS macroceramics were identified. The technological application of these phenomena and principles allowed achieving desirable flexibility, reliability and workability of HTS electric wire. They are the following.

1. The orthorhombic structure and composition of the initial nanosize YBCO ceramic crystals, which defines their superconductivity,[1–3] have to be preserved in the macroceramic body. However, HTS ceramic crystals easily lose one oxygen atom of the crystal lattice in air and during thermal processing, which results in the loss of their initial superconductivity.

   The oxygen was placed back into the YBCO crystals at 420–460°C, thereby restoring their orthorhombic structure and atomic composition, which results in the restoration of superconductivity.
2. As defined by Nobel Prize laureates Ginzburg and Abrikosov,[2,3] superconductive HTS macroceramic leads have to contain two nanophases: HTS ceramic crystal grains (the basic superconductor nanophase) and inorganic nanosized impurities. These impurities provide the vortex pinning effect, which is necessary for intergrain transition of the superconducting electric flux. The flux pinning effect depends on the type and amount of impurity material, as well as on the uniformity of its distribution within the 3D HTS macroceramic body.

   Solidified nanothick glass films act as flux pinning centres. The developed thermochemical nanotechnology resulted in uniform honeycomb-like nanoarchitecture of 3G HTS macroceramics. This architecture provides homogeneous 3D network of the impurity nanophase glass films within the sintered macrosize HTS ceramic body.
3. To avoid interruption of electrical flux in the grain boundary areas of the HTS polycrystalline macroceramic leads, the ceramic body cannot have intergrain nanogaps or micro- and macropores that provide 'weak grain linkages'. Grain alignment makes Josephson junctions of electrons between ceramic crystal grains possible.

   The developed nanofabrication method results in fully dense sintered YBCO composite ceramics providing the required superconductivity.
4. The engineering value of the electric current carrying capability I_E of the polycrystalline macroceramic leads depends on the length of the way for electric flux through all individual crystals within HTS macroleads. A value of I_E can be increased by at least $\sim$100 times if all the HTS ceramic crystals are

uniformly oriented in the direction of the electric flux by *a–b* lattice planes.

The developed method of magnetic grain orientation of freshly coated 3G HTS filaments allowed solving this problem.

5. Sintering of YBCO ceramics is a serious technological problem since the initial crystal structure of the most YBCO crystals has to be retained. This problem was resolved by the development of fast liquid phase sintering method.
6. All ceramic materials are brittle. However, ceramics and glass become flexible if their thickness is below 30 μm. To produce a flexible electric wire, a thin ceramic coating on a flexible metal substrate was applied.

   The developed thermochemical coating of round substrates with diameter 40 μm resulted in ceramic coating thickness of 7–9 μm and a cross-section ratio of substrate filament and YBCO coating layer of ~1 : 1. The flexibility of the coated filaments is practically equal to the metal filaments with minimised bent radiuses.
7. The 3G HTS electric wire is round and in comparison with tape wire provides about five times better magnetic susceptibility, which assures its much more efficient application in coil systems of electric motors, transformers and generator rotors.
8. To be suitable for electrical engineering design and applications, the HTS electric wire has to have precisely equal electromagnetic characteristics along kilometres of length.

   The developed thermochemical coating method is self-controlled and provides repeatability of coating thickness and, therefore, electromagnetic characteristics of the sintered multifilament 3G HTS wire.
9. Reliability is a critical problem of 2G HTS wire, with critical drawbacks in practical usability and workability. The sintering process provides crystal encapsulation in glass films and full densification of YBCO ceramics. This results in the prevention of crystal aging or degradation in contact with air and coolants during long term use. Additionally, it eliminates the necessity for expensive silver protection covers of 2G HTS tapes. All this makes 3G HTS wire durable and less expensive.
10. Inexpensive, reliable and flexible multifilament 3G HTS wire does not have the drawbacks of 1G HTS and 2G HTS wire and can provide enormous engineering, environmental and economic benefits. Table 2 shows that the most of the 22 engineering characteristics of 3G HTS wire exceed the characteristics of much more expensive 1G and 2G HTS wire techniques. This makes 3G HTS nanotechnology the better one and the multifilament 3G HTS-YBCO wire a primary manufacturing candidate.

Conclusion

The developed thermochemical nanofabrication method[13–23] provides silicone polymer assisted phase transformation and nanostructural evolution of YBCO ceramics. These resulted in self-assembly of 3D honeycomb-like nanoarchitecture of the sintered HTS ceramic composite. The produced two-phase nanoarchitecture facilitates superconductivity of the fully dense HTS macroceramics, both bulk and coating.

Sintered YBCO macroceramic samples with superconductive nanoarchitecture demonstrated at LN temperature almost equal inner and intergrain superconductivities and facilitated silver-like electrical conductivity at room temperature. Additionally, the superconductive nanoarchitecture of sintered YBCO ceramic composite makes bulk 3G HTS ceramic leads and coated 3G HTS filaments permanently reliable and durable.

The adhesion coating of metal substrate filaments with the ceramic silicone suspension was developed and resulted in self-controlled constant thickness of flexible and continuous 3G HTS filaments. Dip coating of

Table 2 Engineering characteristics of 1G or oxide ceramic powder loaded in silver tube, 2G or TFD (ceramic film deposition on multimetal template tape) and 3G or ceramic coated and sintered filaments (metal substrate filaments coated with sintered ceramics) HTS wires

#	Characteristics	1G PIT strands	2G TFD tapes	3G coated filaments
1	Substrate and/or cover material	Silver	Multilayer metals	NiCr alloy
2	Geometrical form of wire element	Tube	Tape	Filament
3	Wire forming method	Rolling/drawing	Template deposition	Adhesion coating
4	Thickness of the workable HTS ceramic layer/μm	5–20	0·2–0·3	6–8
5	Magnetic susceptibility	Low	Low	High
6	Cross-section ratio for 'substrate and cover': 'HTS ceramics'	(2–3) : 1	(500–1000) : 1	1 : 1
7	Ratio of production costs to raw material costs	(2–3) : 1	(5–8) : 1	1·1 : 1
8	Capital costs of manufacturing in comparison with each other	5–7	7–12	1
9	Engineering electric current carrying capability of the HTS wire/kA cm^{-2}	1–2	5–10	15–20
10	Insulation of HTS wire	Silver tube	Silver cover tape	Silicone resin
11	Comparison of AC current losses of electric wires	1 (round)	5 (tape)	1 (round)
12	Scrap during prototype wire production	Significant	Significant	Insignificant
13	Estimation of flexibility as max. wire bent/grads	30–50	40–60	140–150
14	Achievable cost/performance ratio of wire (C/P)/$/kA m	200–300	75–100	5–7
15	Quench effects	Significant	Significant	Self-compensated
16	Superconductivity degradation after 3–5 year long service	Remarkable	Remarkable	No degradation
17	Complicity of ceramic grain alignment and orientation	Incomplete	Complete	Complete
18	Possibility to splice two wire pieces	Difficult	Difficult	Easy to do
19	End use applications in electric motors and transformers	Ineffective	Difficult	Effective
20	Electromagnetic shielding of HTS wire	Self-shielded	Difficult	Self-shielded
21	Conductivity of HTS wire at room temperature	As silver metal	As copper metal	As silver metal
22	Long length variability of wire thickness/diameter and superconductivity	Significant	Significant	No variations

substrate filaments, magnetic grain orientation, ceramic silicone composite polymerisation and six-step ceramic firing processes in tube furnace allowed conveyor nanofabrication of 3G HTS-YBCO electric wire filaments. The developed ceramic engineering nanotechnology of 3G HTS-YBCO filaments does not result in innate quality, reliability and workability drawbacks of the mechanically processed 1G and 2G HTS[7–10,38,39] wires.

The cost effective 3G HTS-YBCO electric wire filaments conduct through the entire cross-section ~100 times more electricity while providing flexibility, strength, reliability and workability similar to copper or alumina wire. Thus, YBCO ceramic nanotechnology, flexible and reliable filaments and inexpensive multifilament 3G HTS electric wire with cost/performance ratio C/P=$7/kA m were developed. All this makes 3G HTS wire well competitive with ordinary copper wire.

The manufacturing and use of 3G HTS electric wire can both decrease by three to six times the cost, weight and diameter of cables, motors, transformers and generator rotors and reduce by 50–75% heat losses in electricity transmission and application systems and equipment. This should decrease the total energy consumption by 15–20%, which would eliminate corresponding amounts of green house gas emissions produced by coal power plants.

Acknowledgements

Research conducted with Dr L. Chigirinsky. The author thanks Professors K. Levon, E. Wolf and A. Ulman of the Polytechnic Institute of New York University for the kind support. The superconductivity of the sintered bulk samples of HTS ceramics was measured by Dr A. Ionov at the Institute for Solid State Physics, Russian Academy of Sciences (ISSP RAS), Chernogolovka. The author is very grateful to Dr I. Talmy for valuable discussions of the developed ceramic nanotechnology and Dr E. Medvedovski for editorial suggestions.

References

1. J. G. Bednorz and K. A. Muller: 'Possible high-T_C superconductivity in the Ba–La–Cu–O System', *Z. Phys.*, 1986, **64**, (2), 189–193.
2. K. Fossheim and A. Sudbo: 'Superconductivity physics and applications'; 2004, England, Wiley.
3. N. Khare (ed.): 'Handbook of high-temperature superconductor electronics'; 2003, New York/Basel, Marcel Dekker.
4. C. H. Rosner: 'Emerging 21st century markets and outlook for applied superconducting products', in 'Advanced in cryogenic engineering', (ed. P. Kittel), Vol. 43, 1–24; 1998, New York, Plenum Press.
5. T. Cosmus and M. Parizh: 'Advances in whole-body MRI magnets', *IEEE Trans. Appl. Supercond.*, 2011, **21**, (3), 2104–2109.
6. J. R. Tomson and D. K. Christen: 'Coated conductors: a developing application of high-temperature superconductivity', in 'Superconductivity physics and applications', (ed. K. Fossheim and A. Sudbo), 395–397; 2004, England, Wiley.
7. P. M. Grant: 'Superconductivity and electric power: promises, promises…past, present and future', *IEEE Trans. Appl. Supercond.*, 1997, **7**, 112–133.
8. G. March: 'Time to ripe for superconductivity', *Mater. Today*, 2002, **5**, (4), 46–50.
9. V. A. Maroni: 'Future of high-critical-temperature superconducting ceramics', *Am. Ceram. Soc. Bull.*, 2007, **86**, (6), 29–33.
10. J. L. Mac-Manus-Driscoll and S. C. Wimbush: 'Future directions for cuprate conductors', *IEEE Trans. Appl. Supercond.*, 2011, **21**, (3), 2495–2500.
11. A. Navrotsky: 'Materials and nanotechnology', *MRS Bull.*, 2003, 92–94.
12. Z. Wang, Y. Lin and Z. Zhang (ed.): 'Handbook of nanophase and nanostructured materials', Vol. 1, 'Synthesis'; 2003, New York, Kluwer Academic/Plenum Publishers.
13. A. Rokhvarger: 'Thermochemical nanofabrication of high-temperature superconducting ceramic and multistrand electric wire',*Am. Ceram. Soc. Bull.*, 2010, **8**, 28–33.
14. A. Rokhvarger and L. Chigirinsky: 'Design and nanofabrication of superconductor ceramic strands and customized leads', *Int. J. Appl. Ceram. Technol.*, 2004, **1**, (2), 129–139.
15. A. Rokhvarger and L. Chigirinsky: 'Engineering of superconductive ceramics', *J. Electron. Packag.*, 2004, **126**, (1), 26–33.
16. A. Rokhvarger and L. Chigirinsky: 'Novel nanotechnology of usable superconductor ceramics', *Ceram. Trans.*, 2004, **148**, 163–170.
17. A. Rokhvarger and L. Chigirinsky: 'Unconventional nanoparticle technology of superconductor ceramic articles', *MRS Symp. Proc.*, 2003, **776**, 49–54.
18. A. Rokhvarger and L. Chigirinsky: 'Adhesive-coated HTS wire and other innovative materials', *Ceram. Trans.*, 2003, **140**, 375–384.
19. A. Rokhvarger, L. Chigirinsky and M. Topchiashvili: 'Inexpensive technology of continuous HTS round wire',*Am. Ceram. Soc. Bull.*, 2001, **80**, (12), 37–42.
20. A. E. Rokhvarger and L. A. Chigirinsky: 'Sintered ceramic composite lead with superconductive nano-architecture', US Patent 7 632 784, 2009.
21. A. Rokhvarger and M. Topchiashvili: 'Superconductor composite material', US Patent 6,617,284, 2003.
22. M. Topchiashvili and A. Rokhvarger: 'High temperature superconductor composite material', US Patent 6,239,079, 2001.
23. M. Topchiashvili and A. Rokhvarger: 'Method of conveyor production of high temperature superconductor wire, and other bulk-shaped products using compositions of HTS ceramics, silver, and silicone', US Patent 6,010,983, 2000.
24. '10th anniversary edition product guide', Superconductivity Components Inc., Columbus, OH, USA, http://www.superconductivecomp.com/YBCO123SCPowders.htm.
25. A. Pizzi and K. L. Mittal (eds.): 'Handbook of adhesive technology'; 1994, New York, Marcel Dekker.
26. A. Aymonier and E. Papon: 'Designing soft reactive adhesives by controlling polymer chemistry', *MRS Bull.*, **2003**, 424–427.
27. A. Saxena and G. Aeppli: 'Phase transitions at the nanoscale in functional materials', *Mater. Res. Soc. Bull.*, 2009, **34**, 804–10.
28. K. M. Lang, V. Madhavan, J. E. Hoffman, E. W. Hudson, H. Eisaki, S. Uchida and J. C. Davis: 'Imaging the granular structure of high-T_C superconductivity in underdoped $Bi_2Sr_2CaCu_2O_{8+\delta}$', *Nature*, 2002, **415**, 412–416.
29. K. H. Benneman and J. B. Ketteson (eds.): 'Conventional and high-T_C superconductors. The physics of superconductors', Vol. I; 2003, Berlin/London/New York, Springer-Verlag.
30. G. Hammerl, A. Schmehl, R. R. Schulz, B. Goetz, H. Bielefeldt, C. W. Schneider, H. Hilgenkamp, and J. Mannhart: 'Enhanced supercurrent density in polycrystalline High-T_C superconductors at 77K', *Nature*, 2000, **407**, 162–164.
31. P. Coleman: 'Superconductivity: lifting the gossamer veil', *Nature*, 2003, **424**, 625–626.
32. A. Lanzara, P. V. Bogdanov, X. J. Zhou, S. A. Kellar, D. L. Feng, E. D. Lu, T. Yoshida, H. Eisaki, A. Fujimori, K. Kishio, J. I. Shimoyama, T. Noda, S. Uchida, Z. Hussain and Z. X. Shen: 'Evidence for ubiquitous strong electron–phonon coupling in high-temperature superconductors', *Nature*, 2001, **412**, 510–514.
33. R. W. Hill, C. Proust, L. Taillefer, P. Fournier and R. L. Greene: 'Breakdown of Fermi-liquid theory in a copper–oxide superconductor', *Nature*, 2001, **414**, 711–715.
34. X. J. Zhou, T. Yoshida, A. Lanzara, P. V. Bogdanov, S. A. Kellar, K. M. Shen, W. L. Yang, F. Ronning, T. Sasagawa, T. Kakeshita, T. Noda, H. Eisaki, S. Uchida, C. T. Lin, F. Zhou, J. W. Xiong, W. X. Ti, Z. X. Zhao, A. Fujimori, Z. Hussain and Z.-X. Shen: 'High-temperature superconductors: Universal nodal Fermi velocity', *Nature*, 2003, **423**, 398.
35. Ch. Jooss, J. Albrecht, H. Kuhn, H. Kronmuller and S. Leonhardt: 'Magneto-optical studies of current distributions in high-T_C superconductors', *Rep. Prog. Phys.*, 2002, **65**, 651.

36. A. Polyanskii, R. L. S. Emergo, J. Z. Wu, T. Aytug, D. K. Christen, G. K. Perkins and D. Larbalestier: 'Magneto-optical imaging and electromagnetic study of YBCO vicinal films of variable thickness', *Phys. Rev. B*, 2005, **72B**, 174509.
37. G. A. Levin, K. A. Novak and P. N. Barnes: 'The effects of superconductor-stabilizer interfacial resistance on the quench of a current-carrying coated conductor', *Supercond. Sci. Technol.*, 2010, **23**, 1–8.
38. M. R. Beasley: 'Will higher T_C superconductors be useful? Fundamental issues from the real world', *MRS Bull.*, 2011, **36**, (8), 597–600.
39. A. P. Malozemoff: 'Electric power grid application requirements for superconductors', MRS Bull., 2011, **36**, (8), 601–607.